CJC Chinese Journal of Chemistry 中国化学 · An International Journal

For submission: https://mc.manuscriptcentral.com/cjoc
For published articles: https://onlinelibrary.wiley.com/journal/16147065

Comprehensive Report

Cite this paper: *Chin. J. Chem.* **2021**, *39*, 3071—3078. **DOI: 10.1002/cjoc.202100308**

Seed-mediated Growth of Alloyed Ag-Pd Shells toward Alkyne Semi-hydrogenation Reactions under Mild Conditions†

Yuqin Zheng,[a] Taixing Tan,[b] and Cheng Wang*,[a]

[a] *Tianjin Key Laboratory of Advanced Functional Porous Materials, Institute for New Energy Materials and Low-Carbon Technologies, School of Materials Science and Engineering, Tianjin University of Technology, Tianjin 300384, China*
[b] *Ganjiang Innovation Academy, Chinese Academy of Sciences, Ganzhou, Jiangxi 341000, China*

Keywords

Nanostructures | Alloys | Heterogeneous catalysis | Hydrogenation | Alkynes

Main observation and conclusion

Ag@Ag-Pd$_x$ core-shell nanocomposites with various Ag/Pd ratio were deposited on Ag nanoplates using a seed growth method. When physically loaded on C_3N_4, Ag@Ag-Pd$_{0.077}$/C_3N_4 with optimized Ag/Pd ratio could accomplish high catalytic performance for the semi-hydrogenation of phenylacetylene as well as other aliphatic (both terminal and internal alkynes) alkynes and phenylcycloalkynes containing functional groups (such as ester, hydroxyl, ethyl groups) under room temperature and 1 atm H_2. The alloying and ensemble effects are used to interpret such catalytic performance.

Comprehensive Graphic Content

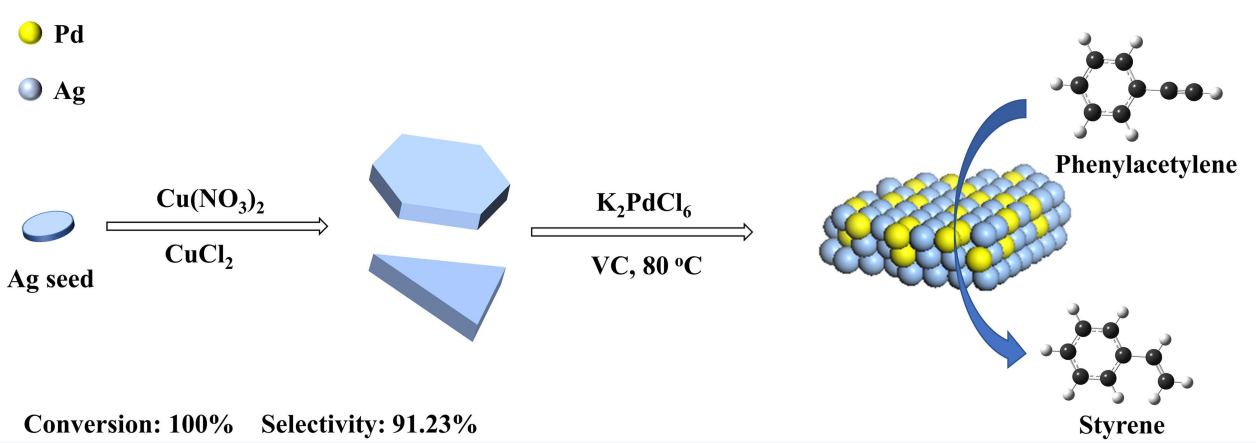

*E-mail: cwang@tjut.edu.cn
† Dedicated to Professor Yitai Qian on the Occasion of His 80th Birthday.

View HTML Article | Supporting Information

Background and Originality Content

Alkenes are important industrial chemical precursors to the industrial synthesis of lots of pharmaceuticals, vitamins, agrochemicals, and polymerization. For example, polystyrene (PS) synthesized from styrene has been widely used to make plastic industrial products. It is worth noting that the removal of even small amounts of phenylacetylene from the styrene feed, because of its toxicity to polymerization, is crucial for producing high quality PS products.[1-2] Therefore, selective semihydrogenation of phenylacetylene is an extremely important and valuable transformation. However, it is difficult to achieve high selectivity and conversion of alkenes in industry since experimental conditions are usually complex and tedious.[1]

For decades, Pd-based catalysts have dominated the hyrogenation of alkynes due to their superior capability in dissociating H_2 and absorbing alkynes.[3-4] However, unmodified Pd catalysts showed poor performance for the transformation of alkynes to alkenes. For a pure Pd surface, the alkynes tend to be converted into alkanes instead of corresponding semi-hydrogenation products, alkenes, since there are sufficient catalytic sites of Pd atoms.[5-6] In addition, the Pd nanoparticles usually undergo a surface reconstruction that leads to the particle sintering during calcination and reactions and subsequently decreases their overall activities. Conventional approaches for enhancing the catalytic selectivity and stability of Pd targeting alkenes via the semi-hydrogenation include controlling the shape of palladium nanocrystals,[7-8] preparing isolated single-atom Pd catalysts,[9-12] using various supports (*e.g*, TiO_2,[13] $Ni(OH)_2$,[14] mpg-C_3N_4,[15] CeO_2,[16-17] Al_2O_3,[18] SiO_2,[19] Fe_3O_4,[20] C,[21-22] N-CNT,[23] HT,[24] COF[25] and MOF[26-31] materials), doping second elements (*e.g*, Pb,[8,32-33] Zn,[34-35] S,[36] P,[37] C,[38-39] Ga,[40-41] In[10,42]), preparing nanocomposites (*e.g*, $CuFe_2O_4$,[43] Cu_2O,[44] ZnO[45]) and using organic modifiers (modifying elements such as N,[46-51] S,[51-55] or P[55]) to poison the active sites. Nearly all these methods could increase the selectivity of Pd as a semi-hydrogenation catalyst by regulating the electronic state (ligand effect)[8,12,15,36] or/and separating the active sites of Pd (ensemble effect).[11,56] The presences of electronic modifiers or/and isolated Pd active sites have been confirmed to be efficient in tuning the adsorption kinetics of the products on the Pd surface, which in turn avoids over-hydrogenation.

In particular, bimetallic alloy catalysts have been widely studied.[57] One of the most attracting properties of these bimetallic alloy nanoparticles is their highly tunable composition and structure, which endow them with superior physical and chemical properties than their single constitutional metallic counterparts in terms of catalytic performance. Lu's group[8] prepared Pd-Pb alloy nanocrystals with tailored composition for semi-hydrogenation of alkynes and found that the introduction of Pb could improve the selectivity of catalyst effectively. Although this strategy can control the composition easily, it has been limited either by complicated synthetic approaches or toxicity of used Pb element. The construction of alloyed surface on core-shell nanostructure could be another effective approach. Yin's group[58] modified Pd surfaces with Au element by constructing Pd-Au alloy surfaces directly on the nanoscale Pd seeds without changing their original surface structures. The above findings clearly show that the exposure of different metal atoms in Pd-based bimetallic nanostructures is an effective strategy to enhance their semi-hydrogenation catalytic performance.[59-60]

Previous studies revealed that the existence of Ag component in a Pd catalyst could significantly facilitate the selective adsorption of alkynes in hydrogenation reactions because the binding energy of alkenes could be decreased on catalyst surface, which is beneficial for the formation of alkenes.[61-66] Zhang's group[61] systematically investigated the molar ratio of Pd/Ag in Pd@Ag core@shell metal nanostructures and found an optimized ratio for the selective semihydrogenation of phenylacetylene. Since most of the reported AgPd bimetallic alloyed catalysts are rich in Pd, they usually suffer from low utilization of the precious noble Pd metal due to its low exposure on the catalyst surface. Here, we designed and fabricated a series of Ag@Ag-Pd core@shell nanocrystals supported on C_3N_4 catalysts using seed-mediated growth method, which has been proven to be a powerful route to synthesize bimetallic core@shell NPs.[60]

Among them, Ag@Ag-$Pd_{0.077}$/C_3N_4 catalyst exhibits the highest catalytic performance for various alkynes, showing nearly 100% conversion and over 90% selectivity to alkenes within 32 h reaction under room temperature and ambient H_2 pressure. The improved catalytic performance of the catalyst is attributed to the combination of the high selectivity of Ag and high activity of Pd by inserting the introduced Pd atoms into the Ag lattice of the Ag nanoplates to generate Ag-Pd alloy shells.

Results and Discussion

Results

Preparation of catalysts. To synthesize Ag nanoplates with loaded Pd on their surfaces, firstly, triangular Ag nanoplates with an average diameter and thickness of about 105 nm and 22 nm (as shown in Figure 1) were synthesized using our previous consecutive seed-mediated synthetic method.[67] Synthetic details could be found in the experimental section. Then the as-prepared Ag nanoplates were used as substrates for the formation of Ag@Ag-Pd alloyed catalysts by reducing K_2PdCl_6 using ascorbic acid as a reductant in aqueous solutions at 80 ^oC . Due to the strong interaction between ascorbic acid and Ag nanoplates, the reduction of K_2PdCl_6 by ascorbic acid allows the formaiton of Pd (0) on the surface of Ag nanoplates. Finally, Ag@Ag-Pd composite nanoplates were physically mixed with C_3N_4 prepared from a conventional method.[68] The introduced C_3N_4 has a large specific surface area[69-71] and more exposed active sites.[72-73] It served as the substrate for anchoring Ag@Ag-Pd composite nanoplates in order to avoid the agglomeration of alloyed nanoplates in subsequent catalytic reaction process.

Characterization of catalysts. In making Ag@Ag-Pd composite nanoplates, 6, 12 and 24 mL 1.0 mmol/L K_2PdCl_6 aqueous solutions were directly added to 40 mL freshly prepared solutions containing 0.125 mmol dispersed Ag nanoplates, separately. After harvesting the products, the molar ratios of Pd to Ag in the three kinds of uniform and monodispersed Ag@Ag-Pd_x, measured by ICP-MS analysis, were 0.041, 0.077 and 0.182 (Table S1), respectively. Their corresponding calculated yields of Pd are 85.5%, 80.1% and 95.1%, respectively. After Pd loading, the thicknesses of the composite nanoplates (about 30 nm) increased and the thickness increases slightly with the increase of Pd loading. Gradual increases of average lateral sizes were also observed as shown in Figure 1 and Figure S1. No isolated Pd nanoparticle was observed for all three products. This might be due to the dispersion of tiny Pd nanoparticles in the solutions that could not be centrifuged together with nanoplates and could also interpret the deviated yields of Pd. This also implies that the surface of Ag triangular nanoplates could serve as a preferential site for the reduction of Pd nanoparticles since most of Pd was deposited on Ag nanoplates. Compared with bare Ag nanoplates (Figure 1a), their surfaces are roughened as a result of the deposition of Pd, suggesting the nonuniform distribution of Pd on their surfaces. Since Ag@Ag-$Pd_{0.077}$ nanoplates exhibit the highest catalytic activity among all investigated catalysts, they were selected for further characterizations.

Under TEM observation (Figure 2a), the nonuniform distribution of Pd becomes more apparent. Our previous work indicates that the top and bottom faces of AgNPs are covered with (111)

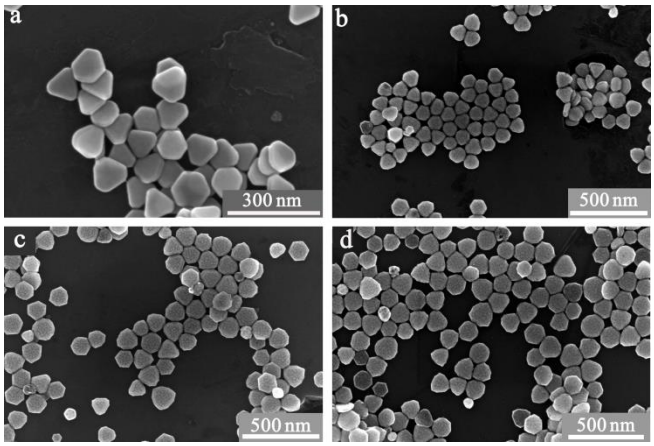

Figure 1 SEM images of primitive Ag (a), Ag@Ag-$Pd_{0.041}$ (b), Ag@Ag-$Pd_{0.077}$ (c) and Ag@Ag-$Pd_{0.182}$ nanaoplates (d).

planes.[62] Under HRTEM (Figure 2b and Figure S2), since the electron beam irradiates along the axis perpendicular to the (111) planes, the observed lattice fringes of 0.25 and 0.24 nm correspond to Ag 1/3(422) and Pd 1/3(422). This observation is due to the presence of stacking faults (or planar defects) in nanoplates.[67,74-76] Two other fringes with d-spacings of 0.248 and 0.246 nm appeared, indicating the formation of AgPd alloys that is believed to be originated from the heat treatment at 80 °C during the Pd reduction process. Elemental mappings of the sample given by energy-dispersive X-ray spectroscopy (EDX) (Figures 2e—2h) revealed that the deposition of Pd took place on the whole Ag surfaces, consistent with the increase of average lateral size and thickness observed in SEM images. The Pd contents in the two Ag-Pd alloys with d-spacings of 0.248 and 0.246 nm are calculated to be 18.2% and 36.4% in molar ratio according to the Vegard's law.[77] The XRD pattern (Figure 2c) is dominated by the (111) peak of FCC Ag as the nanoplates are mainly bound by the (111) planes. There are two additional peaks, ascribed to hexagonal structural defects in Ag nanoplates, adjacent to the (111) peak in the magnified pattern. Besides these two peaks, peaks correlated to the AgPd alloys also appear between Ag (111) and Pd (111) peaks in Figure 2c and Figure 2d. As a result of deposition and uneven distribution of Pd nanoparticles on the surface of Ag nanoplates, a dramatic change of localized surface plasmon resonance (LSPR) occurred. As shown in Figure S3, the primitive Ag nanoplates have four LSPR bands with peaks at 600, 440, 380, and 350 nm, which are indexed to the in-plane dipole, in-plane quadrupole, out-of-plane dipole, and out-of-plane quadrupole resonances, respectively.[67,74] With the deposition of Pd, the in-plane dipole resonance peak of the AgNPs tends to redshift from 600 nm to 680 nm. The in-plane quadrupole resonance peak at 440 nm also redshifts but becomes less prominent.[78-80] The two other out-of-plane resonances could be no longer differentiated caused by the broadening of peaks.[80]

To confirm the formation of alloyed AgPd on the Ag silver nanoplates, X-ray photoelectron spectroscopy (XPS) experiments were also performed to investigate the electronic interaction between Ag and Pd atoms on the catalyst surface. The results showed that the Pd 3d 5/2 peaks for Ag@Ag-$Pd_{0.041}/C_3N_4$, Ag@Ag-$Pd_{0.077}/C_3N_4$ and Ag@Ag-$Pd_{0.182}/C_3N_4$ located below 335 eV were shifted to lower values by approximately 1.1, 0.9 and 1.1 eV as compared to monometallic Pd/C_3N_4 catalyst (Figure 3a). Similarly, the observed Ag 3d 5/2 binding energies for the three alloyed catalysts below 368.0 eV were shifted to lower values by about 0.3, 0.2 and 0.5 eV than the monometallic Ag/C_3N_4 counterpart (Figure 3b). These observations confirm the formation of $AgPd_x$ alloys and suggest electron transfers from Ag to more electronegative Pd atoms within these alloys, which lead to the decrease of the local density of states and shift of the d-band center of the surface Pd. Nevertheless, the formation of $AgPd_x$ alloys in these nanocomposites, as explained by the ligand effects that describe the changes in the chemical properties of the atoms in the surface due to alloying, does not favor the adsorption of acetylene on the alloys' surfaces since the binding energy of acetylene is decreased.[8,36,60,81] It should be pointed out here that, besides forming AgPd alloys with different Ag/Pd ratio, there are also isolated Pd nanoparticles on the surface of all three Ag@Ag-Pd_x/C_3N_4 nanocomposites as evidenced from XPS results in Figure 3a.

Performance of catalysts. The catalytic performance of Ag@Ag-Pd/C_3N_4 (Figure S4) with different Pd/Ag ratio for the selective hydrogenation of phenylacetylene was evaluated in a H_2-filled flask. The hydrogenation reactions were performed in ethanol solvent with the presence of 0.91 mmol of phenylacetylene at room temperature under 1 atm H_2 (Scheme 1). For

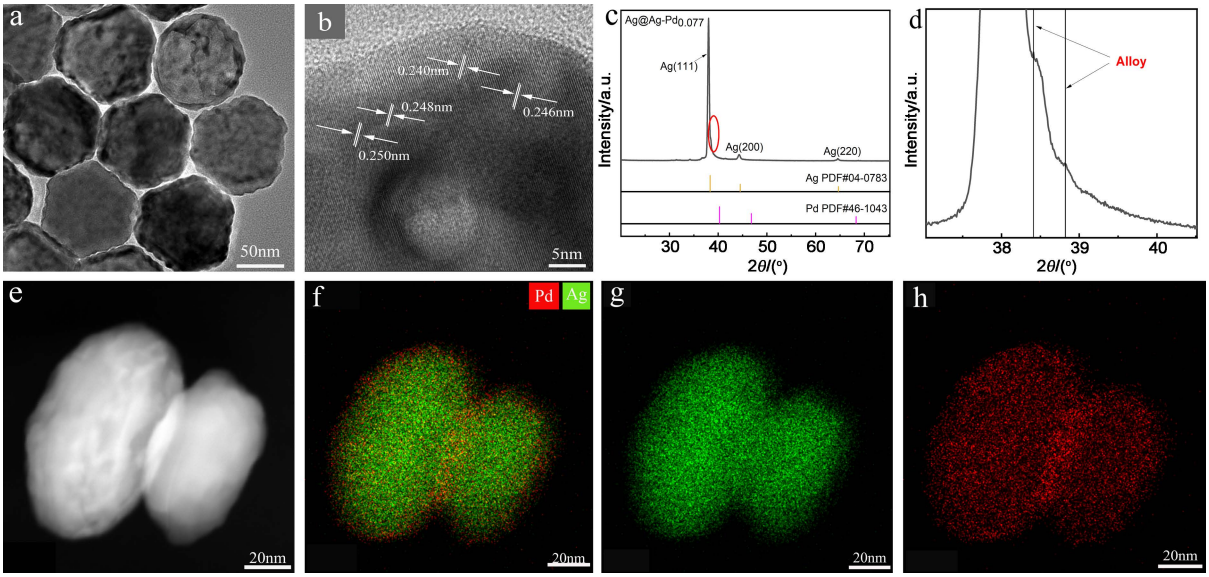

Figure 2 TEM (a), HRTEM (b) images, XRD pattern (c) and its enlarged red ellipse (d) and STEM image and mapping analysis (e—h) of the Ag@Ag-$Pd_{0.077}$ nanoplates.

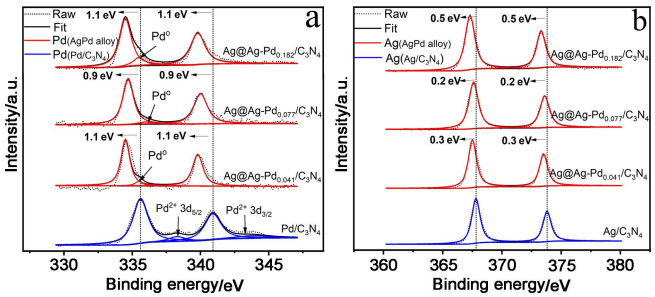

Figure 3 Pd 3d (a) and Ag 3d (b) XPS spectra of Ag/C_3N_4, Pd/C_3N_4, $Ag@Ag\text{-}Pd_{0.041}/C_3N_4$, $Ag@Ag\text{-}Pd_{0.077}/C_3N_4$, $Ag@Ag\text{-}Pd_{0.182}/C_3N_4$ referenced to hydrocarbon C 1s.

Scheme 1 The hydrogenation of phenylacetylene into styrene and ethylbenzene

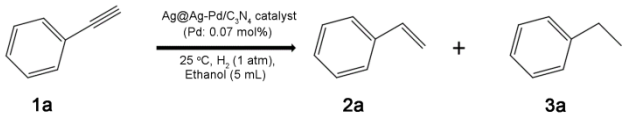

comparison, monometallic Ag/C_3N_4 and Pd/C_3N_4 (Figure S5) catalysts were also prepared using similar protocols. In the cases of catalysts containing Pd, the amounts of Pd added into the reactions were kept almost same. No catalytic activity could be observed (the conversion of phenylacetylene is almost 0%) in the case of pure Ag/C_3N_4 (Figure S6a), while the Pd/C_3N_4 (Figure S6b) achieved a complete conversion (100% conversion of phenylacetylene) within 12 h but showed an extremely poor yield of styrene (almost 0%) because of the over-hydrogenation of styrene to phenylethane. For $Ag@Ag\text{-}Pd_{0.041}/C_3N_4$, nearly 10% conversion of phenylacetylene was obtained, but its selectivity was over 99% (Figure 4a). This suggests that the Ag nanoplates, as substrate and loaded with less amount of Pd, could effectively inhibit the over-hydrogenation of phenylacetylene. When the Pd loading was doubled, $Ag@Ag\text{-}Pd_{0.077}/C_3N_4$ catalyst exhibited a superior catalytic performance. The conversion gradually increased to 100% and the selectivity slightly decreased but still maintained over 90% within 32 h reaction (Figure 4b). Further increasing the Pd loading in $Ag@Ag\text{-}Pd_{0.182}/C_3N_4$, 100% conversion of phenylacetylene could be attained but with a sacrifice of selectivity for styrene (66%) in 12 h (Figure 4c). Under such mild conditions, a lower Pd loading is not sufficient in reducing phenylacetylene, although a high selectivity toward styrene could be achieved, while a higher Pd loading usually cannot guarantee a high selectivity. Therefore, too low or too high Pd loading should be avoided if semi-hyrogenation products were the target products.

The durability of the $Ag@Ag\text{-}Pd_{0.077}/C_3N_4$ catalyst was tested by collecting the catalyst through filtrating after the reaction and being reused in the subsequent running cycles. As shown in Figure S7, the conversion gradually decreases along with an increase of cycling times for five runs. However, the selectivity increased to nearly 100% after 4 runs. The catalyst after reaction exhibited no dramatic change in terms of phase purity, morphology and dispersion as revealed by SEM, TEM, and XRD analysis (Figure S8). Meanwhile, nearly no residual Pd was detected in the supernatant after reaction given from ICP-MS analyses (Table S1), implying that no metal was leached from Ag-Pd alloy surfaces during the catalytic reaction. Interestingly, as shown in Figure 5, 40 mg $Ag@Ag\text{-}Pd_{0.077}/C_3N_4$ catalyst could convert 6.37 mmol phenylacetylene (35 times of the amount of phenylacetylene used in the cycling test) to styrene with selectivity higher than 90%. Although it took nearly 10 d to reach a conversion higher than 90%, the TON was calculated to be 3844.76, which was the highest among catalysts reported in literatures (Table S2). These observations suggested that the catalyst was still efficient once it was not taken out from the catalytic solution. The catalytic activities of $Ag@Ag\text{-}Pd_{0.041}/C_3N_4$ and $Ag@Ag\text{-}Pd_{0.182}/C_3N_4$ samples on the hydrogenation of phenylacetylene with five times of substrate were also tested. Similar performance (combining the conversion and selectivity) to those obtained in Figures 3b and 3d could be attained (Figures S9 and S10). The different catalytic behavior of the $Ag@Ag\text{-}Pd_{0.077}/C_3N_4$ between the cycling test and increased amounts of the phenylacetylene substrate might be interpreted by the composition change of the alloy. In the cycling test, the catalyst with fresh surface was filtered from the catalytic solution and the surficial active Pd atoms might be oxidized during the transfer process. When these oxidized species were subjected to following catalytic reactions, they would be reduced to atomic Pd again, resulting in the change of the original alloy composition. Additionally, migration of surficial Pd atoms to bulk Ag nanoplates might occur during the cycling test and decreases the content of Pd in the $Ag@Ag\text{-}Pd_{0.077}/C_3N_4$, making its Ag/Pd ratio become less (approaching that in $Ag@Ag\text{-}Pd_{0.041}/C_3N_4$) as manifested by the catalytic performance after 5 runs (Figure S11a).

The excellent catalytic performance of $Ag@Ag\text{-}Pd_{0.077}/C_3N_4$ can be further supported using a wide range of alkyne substrates under similar mild conditions (Scheme 2). Aliphatic terminal and internal alkynes could be completely converted to their corresponding alkenes with selectivity near 90% within 12 h running. But for phenylcycloalkynes containing functional groups (such as ester, hydroxyl, ethyl), it took at least 24 h to achieve similar high performance. No corresponding alkanes could be detected after catalytic reactions. The results are summarized in Table 1, confirming that the $Ag@Ag\text{-}Pd_{0.077}/C_3N_4$ is efficient in semi-hydrogenation for a wide range of alkynes.

Discussion

Both experimental and theoretical results revealed that Pd can dissociate hydrogen easily and shows a strong binding of the activated hydrogen (Ha), alkynes and alkenes.[3,82-84] When Ag is

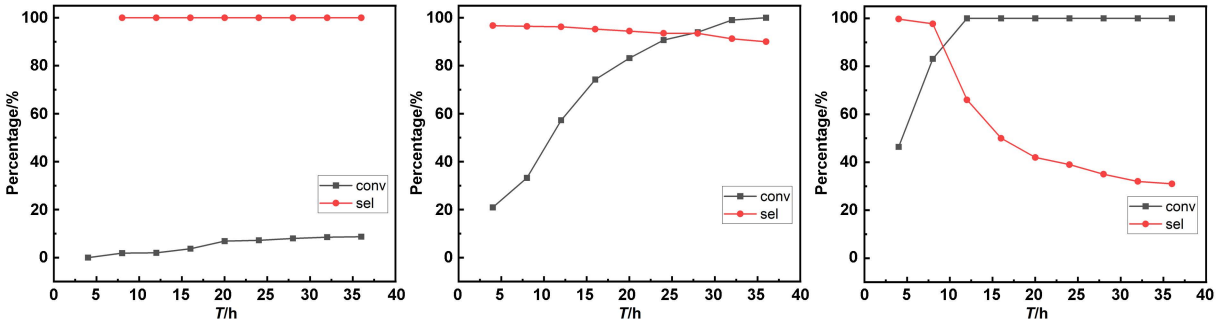

Figure 4 Selectivity and conversion of phenylacetylene into styrene using $Ag@Ag\text{-}Pd_{0.041}/C_3N_4$ (a), $Ag@Ag\text{-}Pd_{0.077}/C_3N_4$ (b), $Ag@Ag\text{-}Pd_{0.182}/C_3N_4$ (c). Reaction conditions: phenylacetylene (0.91 mmol), absolute ethanol (5 mL), H_2 (1 atm), 25 °C, catalysts (Pd/substrate: 0.07 mol%).

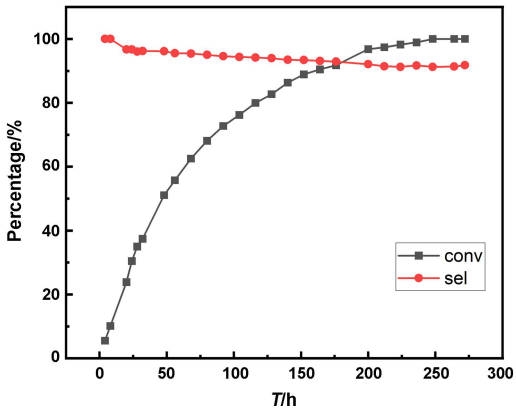

Figure 5 Hydrogenation of 6.37 mmol phenylacetylene over the Ag@Ag-$Pd_{0.077}$/C_3N_4 (40 mg).

Scheme 2 Semihydrogenation of various alkynes

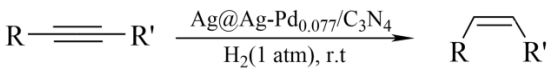

Table 1 The performance of semihydrogenation of various alkynes

Substrate	Product	Time/h	Conv.[a]/%	Sel.[a]/%
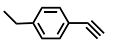	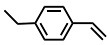	22	100	90
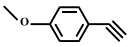	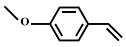	24	100	98
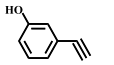		24	100	100
		10	100	96
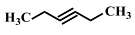	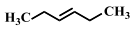	6	100	100
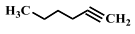	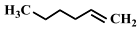	6	100	87.4
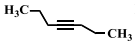	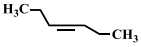	12	100	100

Reaction conditions: Ag@Ag-$Pd_{0.077}$/C_3N_4 (20 mg, Pd/substrate: 0.09%), alkynes (0.91 mmol), EtOH (5 mL). [a]Determined by GC-MS using internal standard technique.

alloyed with Pd on the catalyst surface, an ensemble effect (surface dilution)[11,85] on AgPd alloy surface leads to the formation of single Pd sites or very small Pd clusters. Here, H_2 molecules can be easily dissociated at Pd sites to produce the surface H_a species. Then the generated H_a spills from Pd sites to adjacent Ag metal sites.[65,85-87] It has been revealed that the Ag sites do not adsorb alkynes and alkenes and the binding energy of spilled H_a on them is less than that of Pd sites.[66,88-89] The spilled H_a species on Ag sites tend to flow back to the Pd sites and facilitate the hydrogenation of alkynes or alkenes absorbed on Pd sites. Since Pd site has a higher affinity for alkynes than for alkenes, alkynes prefer to be absorbed and reduced on incompletely covered Pd sites. Therefore, over hydrogenation of phenylacetylene could be suppressed.[36] In addition, the reduction of the ensemble size of Pd and confinement lead to a decreased number of adjacent adsorption sites, block diffusion paths of the organic fragments and limit oligomerization and condensation reactions.[90] These might cause the decrease of overall catalytic activity as manifested by the prolonged reduction time. Meanwhile, Ag nanoplates as growth substrates could suppress the formation of β-palladium hydride (β-PdH) phase, which has been proven to be the key factor for forming alkanes.[8,38,61]

Conclusions

In summary, we developed a seed-mediated growth method to deposit Pd on Ag nanoplates, which form Ag@Ag-Pd_x core-shell nanostructures. When physically mixed with C_3N_4, they were used as catalysts for the semi-hydrogenation of phenylacetylene. Our results showed that a lower Pd loading is not sufficient in reducing phenylacetylene, although a high selectivity toward styrene could be achieved, while a higher Pd loading usually cannot guarantee a high selectivity. With an optimized Ag/Pd ratio, Ag@Ag-$Pd_{0.077}$/C_3N_4 catalyst could convert phenylacetylene completely into styrene with a selectivity being maintained over 90% within 32 h reaction under mild conditions. The catalyst did not show satisfactory durability in the cycling test. But it did give a high TON when the amount of substrate was multiplied by 7 times in a single running test. The improved catalytic performance could be ascribed to the isolated active Pd sites as a result of ensemble effect and the modified electronic structure of Pd after being alloyed with Ag. The poor durability was speculated to be originated from the change of alloy composition in the Ag@Ag-$Pd_{0.077}$/C_3N_4 catalyst during the transfer process in the cycling experiment. A balance between conversion and selectivity toward a wide range of alkynes using Ag@Ag-$Pd_{0.077}$/C_3N_4 catalyst was also attained. The modification approach proposed in this work might be extended to other bimetallic core-shell nanocatalysts for enhancing their performance in heterogeneous catalysis.

Experimental

Materials and apparatus

The reagents, apparatus and methods in the work were listed in Supporting Information.

Preparation of catalysts

Synthesis of Ag nanoplates. Ag seeds are synthesized using the method reported by Yin's group.[91] In a typical process, 5.0 mL Ag seeds, 5.0 mL citrate (25 mmol/L), 2.5 mL PVP (25 mmol/L), 2.5 mL ultrapure water, and 1.5 mL $Cu(NO_3)_2$ (25 mmol/L) were mixed and stirred together in a 100 mL double necked bottle followed by heat treatment at 60 °C. Then, 7.5 mL $AgNO_3$ (10 mmol/L) and 7.5 mL ascorbic acid (10 mmol/L) were simultaneously introduced into the double necked bottle using a peristatic pump. The drop rate was about 0.36 mL/min. After that, 1.5 mL $CuCl_2$ (25 mmol/L) was injected into the reaction solution rapidly. Finally, the same amount of $AgNO_3$ and ascorbic acid were pumped into the double necked bottle.

Synthesis of Ag@Ag-$Pd_{0.077}$ nanoplates. 2.0 mL ascorbic acid (10 mmol/L) was added into 40 mL as-prepared Ag nanoplates solution in a 100 mL single necked bottle followed by heating at 80 °C under constant stirring. On the other hand, 12 mL K_2PdCl_6 (1 mmol/L) and 12 mL ascorbic acid (6.67 mmol/L) were dropped into the reaction solution also using a peristatic pump. The dropping rate was about 0.24 mL/min. The products were collected by centrifugation after being washed with ultrapure water for several times. The purified core@shell nanoplates were redispersed in 10 mL of water for further use.

Synthesis of Ag@Ag-$Pd_{0.041}$ and Ag@Ag-$Pd_{0.182}$ nanoplates. The synthesis was the same as the that of Ag@Ag-$Pd_{0.077}$ except for adding K_2PdCl_6 aq-solution and ascorbic acid with different amount (6 mL and 24 mL, respectively). The products were collected after washing and centrifugation process similar to that of Ag@Ag-$Pd_{0.077}$. The purified core@shell nanoplates were redispersed in 10 mL of water for further use.

Synthesis of Ag@Ag-Pdx/C_3N_4. C_3N_4 was prepared using a method reported by Zhang's group.[68] To prepare the catalysts, purified core@shell nanoplates were mixed with C_3N_4 dissolved in

alcohol. After ultrasonication, the mixtures were stirred and stewed for 48 h, centrifuged and washed with ultrapure water for several times consecutively. The catalysts were dried by Freeze-Dryer for a few days. It should be noticed that the ratio of Ag nanoplates solution to C_3N_4 is 1 mL/5 mg for all core@shell samples.

Synthesis of Ag/C_3N_4. The synthesis was the same as the preparation of Ag@Ag-Pd$_x$/C_3N_4 catalyst except for replacing Ag@Ag-Pd$_x$ core@shell samples by Ag nanoplates.

Synthesis of Pd/C_3N_4. 30 mL K_2PdCl_6 was dropped into 11.35 mg $NaBH_4$ solution dissolved in 50 mL alcohol to allow the synthesis of Pd nanoparticles (corresponding TEM image shown in Figure S5). Then the solution was mixed with 400 mg C_3N_4 dissolved in 50 mL alcohol. Post treatments are similar to those Ag-Pd alloyed catalysts (Ag@Ag-Pd$_x$/C_3N_4)

Catalytic test

Firstly, catalyst powder was dispersed in absolute ethanol under ultrasonication for 5 min. Then, designated amounts of phenylacetylene and catalysts dispersion were mixed in a single neck bottle under constant magnetic stirring. The reaction was triggered once 1 atm H_2 was inlet into the single neck bottle. For cycling test, after each catalytic reaction, the catalyst was removed from the mixture by centrifugation and washed with ethanol for three times. Then fresh phenylacetylene and ethanol were added for further catalytic reaction under the same condition. The filtrates were analyzed by GC-MS with an internal standard to determine the conversion and selectivity.

Supporting Information

The supporting information for this article is available on the WWW under https://doi.org/10.1002/cjoc.202100308.

Acknowledgement

This work was financially supported by the National Key R&D Program of China (2017YFA0700104), the National Natural Science Foundation of China (21911530255) and the State Key Laboratory of Inorganic Synthesis and Preparative Chemistry (2019-6).

References

[1] Tejeda-Serrano, M.; Mon, M.; Ross, B.; Gonell, F.; Ferrando-Soria, J.; Corma, A.; Leyva-Perez, A.; Armentano, D.; Pardo, E. Isolated Fe(III)-O sites catalyze the hydrogenation of acetylene in ethylene flows under front-end industrial conditions. *J. Am. Chem. Soc.* **2018**, *140*, 8827–8832.

[2] Crespo-Quesada, M.; Cardenas-Lizana, F.; Dessimoz, A. L.; Kiwi-Minsker, L. Modern trends in catalyst and process design for alkyne hydrogenations. *ACS Catal.* **2012**, *2*, 1773–1786.

[3] Tierney, H. L.; Baber, A. E.; Kitchin, J. R.; Sykes, E. C. Hydrogen dissociation and spillover on individual isolated palladium atoms. *Phys. Rev. Lett.* **2009**, *103*, 246102–246106.

[4] Mitsui, T.; Rose, M. K.; Fomin, E.; Ogletree, D. F.; Salmeron, M. Dissociative hydrogen adsorption on palladium requires aggregates of three or more vacancies. *Nature* **2003**, *422*, 705–707.

[5] Niu, Y.; Zhang, B.; Luo, J.; Zhang, L.; Chen, C. M.; Su, D. S. Correlation between microstructure evolution of a well-defined cubic palladium catalyst and selectivity during acetylene hydrogenation. *ChemCatChem* **2017**, *9*, 3435–3439.

[6] Crespo-Quesada, M.; Yarulin, A.; Jin, M.; Xia, Y.; Kiwi-Minsker, L. Structure sensitivity of alkynol hydrogenation on shape- and size-controlled palladium nanocrystals: which sites are most active and selective? *J. Am. Chem. Soc.* **2011**, *133*, 12787–12794.

[7] Chung, J.; Kim, C.; Jeong, H.; Yu, T.; Binh, D. H.; Jang, J.; Lee, J.; Kim, B. M.; Lim, B. Selective semihydrogenation of alkynes on shape-controlled palladium nanocrystals. *Chem. Asian J.* **2013**, *8*, 919–925.

[8] Niu, W.; Gao, Y.; Zhang, W.; Yan, N.; Lu, X. Pd-Pb Alloy nanocrystals with tailored composition for semihydrogenation: taking advantage of catalyst poisoning. *Angew. Chem. Int. Ed.* **2015**, *54*, 8271–8274.

[9] Vile, G.; Albani, D.; Nachtegaal, M.; Chen, Z.; Dontsova, D.; Antonietti, M.; Lopez, N.; Perez-Ramirez, J. A stable single-site palladium catalyst for hydrogenations. *Angew. Chem. Int. Ed.* **2015**, *54*, 11265–11269.

[10] Feng, Q.; Zhao, S.; Wang, Y.; Dong, J.; Chen, W.; He, D.; Wang, D.; Yang, J.; Zhu, Y.; Zhu, H.; Gu, L.; Li, Z.; Liu, Y.; Yu, R.; Li, J.; Li, Y. Isolated single-atom Pd sites in intermetallic nanostructures: high catalytic selectivity for semihydrogenation of alkynes. *J. Am. Chem. Soc.* **2017**, *139*, 7294–7301.

[11] Kyriakou, G.; Boucher, M. B.; Jewell, A. D.; Lewis, E. A.; Lawton, T. J.; Baber, A. E.; Tierney, H. L.; Flytzani-Stephanopoulos, M.; Sykes, E. C. Isolated metal atom geometries as a strategy for selective heterogeneous hydrogenations. *Science* **2012**, *335*, 1209–1212.

[12] Huang, F.; Deng, Y.; Chen, Y.; Cai, X.; Peng, M.; Jia, Z.; Ren, P.; Xiao, D.; Wen, X.; Wang, N.; Liu, H.; Ma, D. Atomically dispersed Pd on nanodiamond/graphene hybrid for selective hydrogenation of acetylene. *J. Am. Chem. Soc.* **2018**, *140*, 13142–13146.

[13] Weerachawanasak, P.; Mekasuwandumrong, O.; Arai, M.; Fujita, S.-I.; Praserthdam, P.; Panpranot, J. Effect of strong metal–support interaction on the catalytic performance of Pd/TiO_2 in the liquid-phase semihydrogenation of phenylacetylene. *J. Catal.* **2009**, *262*, 199–205.

[14] Hu, M.; Zhang, J.; Zhu, W.; Chen, Z.; Gao, X.; Du, X.; Wan, J.; Zhou, K.; Chen, C.; Li, Y. 50 ppm of Pd dispersed on $Ni(OH)_2$ nanosheets catalyzing semi-hydrogenation of acetylene with high activity and selectivity. *Nano Res.* **2017**, *11*, 905–912.

[15] Deng, D.; Yang, Y.; Gong, Y.; Li, Y.; Xu, X.; Wang, Y. Palladium nanoparticles supported on mpg-C_3N_4 as active catalyst for semihydrogenation of phenylacetylene under mild conditions. *Green Chem.* **2013**, *15*, 1–7.

[16] Tanimu, A.; Ganiyu, S. A.; Muraza, O.; Alhooshani, K. Palladium nanoparticles supported on ceria thin film for capillary microreactor application. *Chem. Eng. Res. Des.* **2018**, *132*, 479–491.

[17] Li, X.; Song, L.; Gao, D.; Kang, B.; Zhao, H.; Li, C.; Hu, X.; Chen, G. Tandem catalysis of ammonia borane dehydrogenation and phenylacetylene hydrogenation catalyzed by CeO_2 nanotube/Pd@MIL-53(Al). *Chem. - Eur. J.* **2020**, *26*, 4419–4424.

[18] Cordoba, M.; Coloma-Pascual, F.; Quiroga, M. E.; Lederhos, C. R. Olefin purification and selective hydrogenation of alkynes with low loaded Pd nanoparticle catalysts. *Ind. Eng. Chem. Res.* **2019**, *58*, 17182–17194.

[19] Verho, O.; Zheng, H.; Gustafson, K. P. J.; Nagendiran, A.; Zou, X.; Bäckvall, J. E. Application of Pd nanoparticles supported on mesoporous hollow silica nanospheres for the efficient and selective semihydrogenation of alkynes. *ChemCatChem* **2016**, *8*, 773–778.

[20] Uberman, P. M.; Costa, N. J. S.; Philippot, K.; Carmona, R. C.; Dos Santos, A. A.; Rossi, L. M. A recoverable Pd nanocatalyst for selective semi-hydrogenation of alkynes: hydrogenation of benzyl-propargylamines as a challenging model. *Green Chem.* **2014**, *16*, 4566–4574.

[21] Angelica, D. B.; Patrick, D. B.; Johnny, L. N.; Aaron, R. J.; Sergei, A. I.; Jeffrey, T. M.; Ayman, M. K.; Abhaya, K. D. Improved selectivity of carbon-supported palladium catalysts for the hydrogenation of acetylene in excess ethylene. *Appl. Catal. A-Gen.* **2014**, *482*, 108–115.

[22] Li, D. S.; Bing, S. Z.; Wei, Z.; Teschner, D.; Girgsdies, F.; Schlçgl, R.; Dang, S. S. Improved Selectivity by Stabilizing and Exposing Active Phases on Supported Pd Nanoparticles in Acetylene-Selective Hydrogenation. *Chem. - Eur. J.* **2012**, *18*, 14962–14966.

[23] Yue, Q. C.; Wen, Z. F.; Zhou, H. R.; Zhi, J. S.; Jing, H. Z.; Jun, L.; Xue, Z. D.; Xing, G. Z. Tailoring electronic properties and kinetics behaviors of Pd/N-CNTs catalysts for selective hydrogenation of acetylene. *AIChE J.* **2020**, *66*, 16857–16894.

[24] Yu, F. H.; Jia, X. F.; Jun, T. F.; Chi, Y. L.; Peng, F. Y.; Dian, Q. L. Pd nanoparticles on hydrotalcite as an efficient catalyst for partial

hydrogenation of acetylene: Effect of support acidic and basic properties. *J. Catal.* **2015**, *331*, 118–127.

[25] Li, J. H.; Yu, Z. W.; Gao, Z.; Li, J. Q.; Tao, Y.; Xiao, Y. X.; Yin, W. H.; Fan, Y. L.; Jiang, C.; Sun, L. J.; Luo, F. Ultralow-content palladium dispersed in covalent organic framework for highly efficient and selective semihydrogenation of alkynes. *Inorg. Chem.* **2019**, *58*, 10829–10836.

[26] Bakuru, V. R.; Samanta, D.; Maji, T. K.; Kalidindi, S. B. Transfer hydrogenation of alkynes into alkenes by ammonia borane over Pd-MOF catalysts. *Dalton Trans.* **2020**, *49*, 5024–5028.

[27] Wu, H. Q.; Huang, L.; Li, J. Q.; Zheng, A. M.; Tao, Y.; Yang, L. X.; Yin, W. H.; Luo, F. Pd@Zn-MOF-74: restricting a guest molecule by the open-metal site in a metal-organic framework for selective semihydrogenation. *Inorg. Chem.* **2018**, *57*, 12444–12447.

[28] Peng, L.; Zhang, J.; Yang, S.; Han, B.; Sang, X.; Liu, C.; Yang, G. The ionic liquid microphase enhances the catalytic activity of Pd nanoparticles supported by a metal–organic framework. *Green Chem.* **2015**, *17*, 4178–4182.

[29] Bakuru, V. R.; Velaga, B.; Peela, N. R.; Kalidindi, S. B. Hybridization of Pd nanoparticles with UiO-66(Hf) metal-organic framework and the effect of nanostructure on the catalytic properties. *Chem. - Eur. J.* **2018**, *24*, 15978–15982.

[30] Choe, K.; Zheng, F.; Wang, H.; Yuan, Y.; Zhao, W.; Xue, G.; Qiu, X.; Ri, M.; Shi, X.; Wang, Y.; Li, G.; Tang, Z. Fast and selective semihydrogenation of alkynes by palladium nanoparticles sandwiched in metal-organic frameworks. *Angew. Chem. Int. Ed.* **2020**, *59*, 3650–3657.

[31] Tao, Y.; Wu, H. Q.; Li, J. Q.; Yang, L. X.; Yin, W. H.; Luo, M. B.; Luo, F. Applying MOF(+) technique for in situ preparation of a hybrid material for hydrogenation reaction. *Dalton Trans.* **2018**, *47*, 14889–14892.

[32] Anderson, J.; Mellor, J.; Wells, R. Pd catalysed hexyne hydrogenation modified by Bi and by Pb. *J. Catal.* **2009**, *261*, 208–216.

[33] Liu, J.; Zhu, Y.; Liu, C.; Wang, X.; Cao, C.; Song, W. Excellent selectivity with high conversion in the semihydrogenation of alkynes using palladium-based bimetallic catalysts. *ChemCatChem* **2017**, *9*, 4053–4057.

[34] Mashkovsky, I. S.; Markov, P. V.; Bragina, G. O.; Baeva, G. N.; Rassolov, A. V.; Bukhtiyarov, A. V.; Prosvirin, I. P.; Bukhtiyarov, V. I.; Stakheev, A. Y. PdZn/α-Al_2O_3 catalyst for liquid-phase alkyne hydrogenation: effect of the solid-state alloy transformation into intermetallics. *Mendeleev Commun.* **2018**, *28*, 152–154.

[35] Hui, R. Z.; Xiao, F. Y.; Lin, L.; Xiao, Y. L.; Yan, Q. H.; Xiao, l. P.; Ai, Q. W.; Jun, L.; Tao, Z. PdZn intermetallic nanostructure with Pd−Zn−Pd ensembles for highly active and chemoselective semi-hydrogenation of acetylene. *ACS Catal.* **2016**, *6*, 1054−1061.

[36] Albani, D.; Shahrokhi, M.; Chen, Z.; Mitchell, S.; Hauert, R.; Lopez, N.; Perez-Ramirez, J. Selective ensembles in supported palladium sulfide nanoparticles for alkyne semi-hydrogenation. *Nat. Commun.* **2018**, *9*, 2634–2645.

[37] Ren, M.; Li, C.; Chen, J.; Wei, M.; Shi, S. Preparation of a ternary Pd–Rh–P amorphous alloy and its catalytic performance in selective hydrogenation of alkynes. *Catal. Sci. Technol.* **2014**, *4*, 1920–1924.

[38] Guo, R.; Chen, Q.; Li, X.; Liu, Y.; Wang, C.; Bi, W.; Zhao, C.; Guo, y.; Jin, M. PdCx nanocrystals with tunable compositions for alkyne semihydrogenation. *J. Mater. Chem. A* **2019**, *7*, 4714–4720.

[39] Zhang, L.; Ding, Y.; Wu, K. H.; Niu, Y.; Luo, J.; Yang, X.; Zhang, B.; Su, D. Pd@C core-shell nanoparticles on carbon nanotubes as highly stable and selective catalysts for hydrogenation of acetylene to ethylene. *Nanoscale* **2017**, *9*, 14317−14321.

[40] Marc, A.; Kirill, K.; Malte, B.; Detre, T.; Yuri, G.; Robert, S. Pd-Ga intermetallic compounds as highly selective semihydrogenation catalysts. *J. Am. Chem. Soc.* **2010**, *132*, 14745–14747.

[41] Armbruster, M.; Wowsnick, G.; Friedrich, M.; Heggen, M.; Cardoso-Gil, R. Synthesis and catalytic properties of nanoparticulate intermetallic Ga-Pd compounds. *J. Am. Chem. Soc.* **2011**, *133*, 9112–9118.

[42] Yue, Q. C.; Zhi, J. S.; Yian, Z.; Xing, G. Z.; De, C. Selective hydrogenation of acetylene over Pd-In/Al_2O_3 catalyst: promotional effect of indium and composition-dependent performance. *ACS Catal.* **2017**, *7*, 7835−7846.

[43] Lee, K. H.; Lee, B.; Lee, K. R.; Yi, M. H.; Hur, N. H. Dual Pd and $CuFe_2O_4$ nanoparticles encapsulated in a core/shell silica microsphere for selective hydrogenation of arylacetylenes. *Chem. Commun.* **2012**, *48*, 4414–4416.

[44] Yang, S.; Cao, C.; Peng, L.; Zhang, J.; Han, B.; Song, W. A Pd-Cu_2O nanocomposite as an effective synergistic catalyst for selective semi-hydrogenation of the terminal alkynes only. *Chem. Commun.* **2016**, *52*, 3627–3630.

[45] Tian, H.; Huang, F.; Zhu, Y.; Liu, S.; Han, Y.; Jaroniec, M.; Yang, Q.; Liu, H.; Lu, G. Q. M.; Liu, J. The development of yolk-shell-structured Pd&ZnO@carbon submicroreactors with high selectivity and stability. *Adv. Funct. Mater.* **2018**, *28*,1801737.

[46] Kuwahara, Y.; Kango, H.; Yamashita, H. Pd nanoparticles and aminopolymers confined in hollow silica spheres as efficient and reusable heterogeneous catalysts for semihydrogenation of alkynes. *ACS Catal.* **2019**, *9*, 1993−2006.

[47] Wu, J.; Wang, K. J.; Li, Y.; Yu, P. Semihydrogenation of phenylacetylene catalyzed by palladium nanoparticles supported on organic group modified silica. *Adv. Mater. Res.* **2011**, *233–235*, 2109–2112.

[48] Karakhanov, E. A.; Maximov, A. L.; Zolotukhina, A. V. Selective semihydrogenation of phenyl acetylene by Pd nanocatalysts encapsulated into dendrimer networks. *Mol. Catal.* **2019**, *469*, 98–110.

[49] Karakhanov, E.; Maximov, A.; Kardasheva, Y.; Semernina, V.; Zolotukhina, A.; Ivanov, A.; Abbott, G.; Rosenberg, E.; Vinokurov, V. Pd nanoparticles in dendrimers immobilized on silica-polyamine composites as catalysts for selective hydrogenation. *ACS Appl. Mater. Interfaces* **2014**, *6*, 8807–8816.

[50] Mizugaki, T.; Murata, M.; Fukubayashi, S.; Mitsudome, T.; Jitsukawa, K.; Kaneda, K. PAMAM dendron-stabilised palladium nanoparticles: effect of generation and peripheral groups on particle size and hydrogenation activity. *Chem. Commun.* **2008**, 241–243.

[51] Moreno, M.; Ibanez, F. J.; Jasinski, J. B.; Zamborini, F. P. Hydrogen reactivity of palladium nanoparticles coated with mixed monolayers of alkyl thiols and alkyl amines for sensing and catalysis applications. *J. Am. Chem. Soc.* **2011**, *133*, 4389–4397.

[52] Takahashi, Y.; Hashimoto, N.; Hara, T.; Shimazu, S.; Mitsudome, T.; Mizugaki, T.; Jitsukawa, K.; Kaneda, K. Highly efficient Pd/SiO_2–dimethyl sulfoxide catalyst system for selective semihydrogenation of alkynes. *Chem. Lett.* **2011**, *40*, 405–407.

[53] Zhao, X.; Zhou, L.; Zhang, W.; Hu, C.; Dai, L.; Ren, L.; Wu, B.; Fu, G.; Zheng, N. Thiol treatment creates selective palladium catalysts for semihydrogenation of internal alkynes. *Chem* **2018**, *4*, 1080–1091.

[54] Mitsudome, T.; Takahashi, Y.; Ichikawa, S.; Mizugaki, T.; Jitsukawa, K.; Kaneda, K. Metal-ligand core-shell nanocomposite catalysts for the selective semihydrogenation of alkynes. *Angew. Chem. Int. Ed.* **2013**, *52*, 1481–1485.

[55] Yun, S.; Lee, S.; Yook, S.; Patel, H. A.; Yavuz, C. T.; Choi, M. Cross-linked “poisonous” polymer: thermochemically stable catalyst support for tuning chemoselectivity. *ACS Catal.* **2016**, *6*, 2435–2442.

[56] Karakhanov, E. A.; Maximov, A. L.; Zolotukhina, A. V.; Yatmanova, N.; Rosenberg, E. Alkyne hydrogenation using Pd-Ag hybrid nanocatalysts in surface-immobilized dendrimers. *Appl. Organomet. Chem.* **2015**, *29*, 777–784.

[57] Li, C.; Shao, Z.; Pang, M.; Williams, C. T.; Zhang, X.; Liang, C. Carbon nanotubes supported mono- and bimetallic Pt and Ru catalysts for selective hydrogenation of phenylacetylene. *Ind. Eng. Chem. Res.* **2012**, *51*, 4934–4941.

[58] Li, X.; Wang, Z.; Zhang, Z.; Yang, G.; Jin, M.; Chen, Q.; Yin, Y. Construction of Au–Pd alloy shells for enhanced catalytic performance toward alkyne semihydrogenation reactions. *Mater. Horizons.* **2017**, *4*, 584–590.

[59] Zhang, Z.; Liu, Y.; Chen, B.; Gong, Y.; Gu, L.; Fan, Z.; Yang, N.; Lai, Z.; Chen, Y.; Wang, J.; Huang, Y.; Sindoro, M.; Niu, W.; Li, B.; Zong, Y.; Yang, Y.; Huang, X.; Huo, F.; Huang, W.; Zhang, H. Submonolayered Ru deposited on ultrathin Pd nanosheets used for enhanced catalytic

applications. *Adv. Mater.* **2016**, *28*, 10282–10286.
[60] Chen, L.; Huang, B.; Qiu, X.; Wang, X.; Luque, R.; Li, Y. Seed-mediated growth of MOF-encapsulated Pd@Ag core-shell nanoparticles: toward advanced room temperature nanocatalysts. *Chem. Sci.* **2016**, *7*, 228–233.
[61] Song, S.; Li, K.; Pan, J.; Wang, F.; Li, J.; Feng, J.; Yao, S.; Ge, X.; Wang, X.; Zhang, H. Achieving the trade-off between selectivity and activity in semihydrogenation of alkynes by fabrication of (asymmetrical Pd@Ag core)@(CeO_2 shell) nanocatalysts via autoredox reaction. *Adv. Mater.* **2017**, *29,* 1605332.
[62] Zhang, S.; Xia, Z.; Chen, X.; Gao, W.; Qu, Y. Selective semihydrogenation of phenylacetylene to styrene catalyzed by alloyed palladium/gold catalysts anchored on cerium oxide. *ChemNanoMat* **2018**, *4*, 472–476.
[63] Wei, H. H.; Yen, C. H.; Lin, H. W.; Tan, C. S. Synthesis of bimetallic PdAg colloids in CO_2-expanded hexane and their application in partial hydrogenation of phenylacetylene. *J. Supercrit. Fluids* **2013**, *81*, 1–6.
[64] Mitsudome, T.; Urayama, T.; Yamazaki, K.; Maehara, Y.; Yamasaki, J.; Gohara, K.; Maeno, Z.; Mizugaki, T.; Jitsukawa, K.; Kaneda, K. Design of core-Pd/shell-Ag nanocomposite catalyst for selective semihydrogenation of alkynes. *ACS Catal.* **2015**, *6*, 666–670.
[65] Pei, G. X.; Liu, X. Y.; Wang, A.; Lee, A. F.; Isaacs, M. A.; Li, L.; Pan,X.; Yang, X.; Wang, X.; Tai, Z.; Wilson, K.; Zhang, T. Ag alloyed Pd single-atom catalysts for efficient selective hydrogenation of acetylene to ethylene in excess ethylene. *ACS Catal.* **2015**, *5*, 3717–3725.
[66] Studt, F.; Abild-Pedersen, F.; Bligaard, T.; Sorensen, R. Z.; Christensen, C. H.; Norskov, J. K. On the role of surface modifications of palladium catalysts in the selective hydrogenation of acetylene. *Angew. Chem. Int. Ed.* **2008**, *47*, 9299–9302.
[67] Tan, T.; Yao, L.; Liu, H.; Li, C.; Wang, C. Precise control of the lateral and vertical growth of two-dimensional Ag nanoplates. *Chem. - Eur. J.* **2017**, *23*, 10001–10006.
[68] Dai, Y.; Li, C.; Shen, Y.; Lim, T.; Xu, J.; Li, Y.; Niemantsverdriet, H.; Besenbacher, F.; Lock, N.; Su, R. Light-tuned selective photosynthesis of azo- and azoxy-aromatics using graphitic C_3N_4. *Nat. Commun.* **2018**, *9*, 60–67.
[69] Shuang, Y. B.; Wei, W. Y.; Ying, J. W.; Yong, S. Y.; Yin, Y. S. Highly efficient and ultrafast removal of Cr(VI) in aqueous solution to ppb level by poly(allylamine hydrochloride) covalently cross-linked amino-modified graphene oxide. *J. Hazard. Mater.* **2021**, *409*, 124470.
[70] Ying, J. W.; Shuang, Y. B.; Ye, Q. L.; Wei, W. Y.; Yong, S. Y.; Ming, F.; Ke, F. L. Efficient photocatalytic reduction of Cr(VI) in aqueous solution over CoS_2/g-C_3N_4-rGO nanocomposites under visible light. *Appl. Surf. Sci.* **2020**, *510*, 145495.
[71] Shuo, G.; Wei, W. Y.; Yong, S. Y. Building MoS_2/S-doped g-C_3N_4 layered heterojunction electrocatalysts for efficient hydrogen evolution reaction. *J. Catal.* **2019**, *375*, 441–447.
[72] Xin, Y. L.; Hu, L.; Ying, J. W.; Wei, W. Y.; Yong, S. Y. Nitrogen-rich g-C_3N_4@AgPd Mott-Schottky heterojunction boosts photocatalytic hydrogen production from water and tandem reduction of NO_3^- and NO_2^-. *J. Colloid Interface Sci.* **2021**, *581*, 619–626.
[73] Hu, L.; Xin, Y. L.; Wei, W. Y.; Meng, Q. S.; Shuo, G.; Chao, Y.; Bo, S.; Yong, S. Y. Photocatalytic dehydrogenation of formic acid promoted by a superior PdAg@g-C_3N_4 Mott–Schottky heterojunction. *J. Mater. Chem. A* **2019**, *7*, 2022–2026.
[74] Tan, T.; Tian, C.; Ren, Z.; Yang, J.; Chen, Y.; Sun, L.; Li, Z.; Wu, A.; Yin, J.; Fu, H. LSPR-dependent SERS performance of silver nanoplates with highly stable and broad tunable LSPRs prepared through an improved seed-mediated strategy. *Phys. Chem. Chem. Phys.* **2013**, *15*, 21034–21042.
[75] Lofton, C.; Sigmund, W. Mechanisms controlling crystal habits of gold and silver colloids. *Adv. Funct. Mater.* **2005**, *15*, 1197–1208.
[76] Aherne, D.; Ledwith, D. M.; Gara, M.; Kelly, J. M. Optical properties and growth aspects of silver nanoprisms produced by a highly reproducible and rapid synthesis at room temperature. *Adv. Funct. Mater.* **2008**, *18*, 2005–2016.
[77] Denton, A. R.; Ashcroft, N. W. Vegard's law. *Phys. Rev. A* **1991**, *43*, 3161–3164.
[78] Li, B.; Long, R.; Zhong, X.; Bai, Y.; Zhu, Z.; Zhang, X.; Zhi, M.; He, J.; Wang, C.; Li, Z. Y.; Xiong, Y. Investigation of size-dependent plasmonic and catalytic properties of metallic nanocrystals enabled by size control with HCl oxidative etching. *Small* **2012**, *8*, 1710–1716.
[79] Tan, T.; Zhang, S.; Wang, C. Branched Ag nanoplates: synthesis dictated by suppressing surface diffusion and catalytic activity for nitrophenol reduction. *CrystEngComm* **2017**, *19*, 6339–6346.
[80] Zhang, Q.; Hu, Y.; Guo, S.; Goebl, J.; Yin, Y. Seeded growth of uniform Ag nanoplates with high aspect ratio and widely tunable surface plasmon bands. *Nano Lett.* **2010**, *10*, 5037–5042.
[81] Chen, Y.; Zhu, Q. L.; Tsumori, N.; Xu, Q. Immobilizing highly catalytically active noble metal nanoparticles on reduced graphene oxide: a non-noble metal sacrificial approach. *J. Am. Chem. Soc.* **2015**, *137*, 106–109.
[82] Mei, D.; Sheth, P.; Neurock, M.; Smith, C. First-principles-based kinetic Monte Carlo simulation of the selective hydrogenation of acetylene over Pd(111). *J. Catal.* **2006**, *242*, 1–15.
[83] Sheth, P. A.; Neurock, M.; Smith, C. M. A first-principles analysis of acetylene hydrogenation over Pd(111). *J. Phys. Chem. B* **2003**, *107*, 2009–2017.
[84] Paul, J. F.; Sautet, P. Density-functional periodic study of the adsorption of hydrogen on a palladium (111) surface. *Phys. Rev. B* **1996**, *53*, 8015–8027.
[85] Slanac, D. A.; Hardin, W. G.; Johnston, K. P.; Stevenson, K. J. Atomic ensemble and electronic effects in Ag-rich AgPd nanoalloy catalysts for oxygen reduction in alkaline media. *J. Am. Chem. Soc.* **2012**, *134*, 9812–9819.
[86] Li, Q.; Song, L.; Pan, L.; Zhuang, X.; Ling, M.; Duan, L. Ensemble and ligand effects on the acetylene adsorption on ordered PdAgPd(100) surface alloys investigated by periodic DFT study. *Phys. Chem. Chem. Phys.* **2013**, *15*, 20345—20353.
[87] Azad, S.; Kaltchev, M.; Stacchiola, D.; Wu, G.; Tysoe, W. T. On the reaction pathway for the hydrogenation of acetylene and vinylidene on Pd(111). *J. Phys. Chem. B* **2000**, *104*, 3107–3115.
[88] Li, Q.; Qin, Y.; Tan, D.; Xie, Y.; Lv, M.; Song, L. Theoretical investigation of conversion between different C_2H_x species over Pd–Ag/Pd(100) surface alloys: influence on the selectivity and transformation of carbonaceous species. *New J. Chem.* **2018**, *42*, 19827–19836.
[89] Li, Q.; Ma, Y.; Qi, H.; Mo, Z.; Zhang, X.; Song, L. Impact of surface arrangement and composition on ethylene adsorption over Pd–Ag surface alloys: a computational study. *RSC Adv.* **2016**, *6*, 70932–70942.
[90] Vilé, G.; Albani, D.; Almora-Barrios, N.; López, N.; Pérez-Ramírez, J. Advances in the design of nanostructured catalysts for selective hydrogenation. *ChemCatChem* **2016**, *8*, 21–33.
[91] Zhang, Q.; Li, N.; Goebl, J.; Lu, Z.; Yin, Y. A systematic study of the synthesis of silver nanoplates: is citrate a "magic" reagent? *J. Am. Chem. Soc.* **2011**, *133*, 18931–18939.

Manuscript received: April 29, 2021
Manuscript revised: July 30, 2021
Manuscript accepted: August 10, 2021
Accepted manuscript online: August 14, 2021
Version of record online: XXXX, 2021

